Journal of Catalysis 428 (2023) 115194

Contents lists available at ScienceDirect

Journal of Catalysis

journal homepage: www.elsevier.com/locate/jcat

Investigation of Rh/NR_3 catalytic systems in sequential stages of reductive hydroformylation engaging *in situ* X-ray absorption spectroscopy

D.N. Gorbunov [a,*], M.V. Nenasheva [a], I.A. Baravoi [a], A.A. Guda [b,*], V.G. Vlasenko [c], A.L. Trigub [e], V.V. Shapovalov [b], A.D. Zagrebaev [b], B.O. Protsenko [b], A.V. Soldatov [b], E.R. Naranov [d], A.L. Maximov [d]

[a] *Lomonosov Moscow State University, Faculty of Chemistry, 119234, Leninskie Gory, 1, 3, Moscow, Russia*
[b] *The Smart Materials Research Institute, Sladkova 178/24, 344090 Rostov-on-Don, Russia*
[c] *Institute of Physics, Southern Federal University, Stachki Ave., 194, 344090 Rostov-on-Don, Russia*
[d] *Topchiev Institute of Petrochemical Synthesis, Russian Academy of Sciences, Leninskiy Prospect 29, Moscow 119991, Russia*
[e] *National Research Center "Kurchatov Institute", Akademika Kurchatova pl. 1, 123182 Moscow, Russia*

ARTICLE INFO

Keywords:
Reductive hydroformylation
Rhodium complexes
X-ray absorption spectroscopy
XANES
EXAFS
In situ measurements
Amines

ABSTRACT

Nowadays reductive hydroformylation over Rh/NR_3 catalysts is of great interest to both industry and academia, however, some of its aspects remain controversial or unclear, including those which might turn essential for developing new active catalysts and optimization of parameters. In this work, we studied in depth separately both stages of the process – hydroformylation of olefins and hydrogenation of aldehydes, – and estimated the role of the amine structure in them. Also, for the first time, we investigated Rh/NR_3 catalytic system under the reaction conditions by *in situ* XAS method to gain the additional structural information, and observed the correlation of the obtained data with the results of catalytic experiments. Catalytic and *in situ* XAS measurements shown that tertiary amines suppress Rh clusterization, forming species of lower nuclearity. These Rh/amine species may include both charged and uncharged ones. The addition of amines, which are effective promotors of the hydrogenation step, decelerates hydroformylation, presumably, through the formation of amine containing Rh complexes.

1. Introduction

Reductive hydroformylation is a simple way to produce primary alcohols from olefins through a one-step process (Fig. 1).

Nowadays, only Co-phosphine system is used for it in industry, however, it requires harsh conditions (5–10 MPa, 160–200 °C) [1] and has comparatively low selectivity in oxo-products. For hydroformylation, Rh complexes are used for better productivity in milder conditions, but no Rh-based system for the direct alcohol synthesis is applied. At the same time, several types of Rh systems are known to catalyze reductive hydroformylation, including those with aliphatic phosphine [2,3] and N-containing phosphine ligands [4,5], bimetallic Rh-Ru ones [6,7], and some others [8]. One of the most promising of them is Rh/NR_3, where R = alkyl [9]. Tertiary amines are available and cheap substances, resilient to water and oxygen. Many of them are less hazardous than the phosphorus (III) compounds, widely used as hydroformylation ligands and their precursors. Rh/NR_3 systems were successfully applied for reductive hydroformylation of various substrates including dienes [10,11], vegetable oils [12,13], allyl ether [14]; several biphasic systems [15–19] and solid catalysts [11,20,21] of this type were reported; they were also tested in the reductive hydroformylation under WGSR conditions [22]. Reductive hydroformylation over Rh/NR_3 catalysts has been studied since 1970s [23,24], however, some of its aspects remain unclear. The results of catalytic experiments suggest that Rh must be bonded to amine in the active species, but such complexes were not registered spectroscopically. Also, most of the studies focused on the integral tandem reaction and an effect of various parameters on the alcohol yields in it, while, being a two-stage process in this case, reductive hydroformylation is a combination of the two consecutive reactions – hydroformylation of olefins and hydrogenation of aldehydes, so for its deeper understanding and finer tuning, the stages should be studied separately.

* Corresponding authors.
E-mail addresses: gorbunovdn@petrol.chem.msu.ru (D.N. Gorbunov), guda@sfedu.ru (A.A. Guda).

https://doi.org/10.1016/j.jcat.2023.115194
Received 13 September 2023; Received in revised form 25 October 2023; Accepted 30 October 2023
Available online 31 October 2023

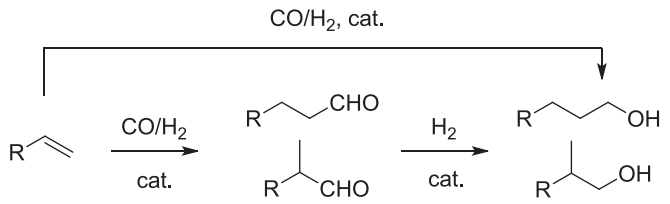

Fig. 1. Tandem hydroformylation-hydrogenation of olefins.

Here, we present new insights into the process of Rh/NR_3-catalyzed reductive hydroformylation deduced from the *in situ* X-ray absorption examination of the system and catalytic experiments. In the first part of the work, we studied the catalytic properties of homogeneous Rh complexes with different amine ligands in olefin hydroformylation and aldehyde hydrogenation as separated stages of tandem reductive hydroformylation. Then we investigated interactions between Rh precursor and amine ligands under ambient and the reaction conditions (90℃, 3.0 MPa) using *in situ* X-ray absorption spectroscopy. Based on catalytic and spectroscopic studies, we proposed the scheme of possible transformations of Rh complexes and discussed the influence of amines on these transformations as well as on catalytic activity of obtained Rh species in hydroformylation and aldehyde hydrogenation.

2. Experimental and computational details

2.1. Experimental details

The reagents: amines – N,N-Dimethylbenzylamine (DMBA, ≥ 99 %, Sigma Aldrich), N,N-Dimethylcyclohexylamine (DMCHA, 99 %, Sigma Aldrich), N,N-Dimethylisopropylamine (DMPA, ≥ 99 %, Sigma Aldrich), Tripropylamine (NPr_3, ≥ 98 %, Sigma Aldrich), 1,4-Dimethylpiperazine (1,4-DMP, 98 %, Sigma Aldrich), Triisobutylamine (iBu_3N, 98 %, Sigma Aldrich), 2,4,6-Tris(dimethylaminomethyl)phenol (DMP-30, 95 %, Sigma Aldrich), N,N-Dimethylethylamine (Me_2EtN, ≥ 99 %, Sigma Aldrich), Hexamethylenetetramine (Urotropin, for synthesis, Sigma Aldrich), N,N,N′,N′-Tetramethyl-1,6-hexanediamine (TMHDA, 99 %, Sigma Aldrich), N,N,N′,N′-Tetramethylethylenediamine (TMEDA, 99.5 %, Sigma Aldrich), Pyridine (≥99 %, Sigma Aldrich), 1,4-Diazabicyclo [2.2.2]octane (1,4-DABCO, for synthesis, Sigma Aldrich), N-Methylpyrrolidine (NMP-dine, 97 %, Sigma Aldrich), N-Methylpyrrolidone (NMP-done, 99 %, Sigma Aldrich), Triethylamine (NEt_3, 99.5 %, Sigma Aldrich), hexene-1 (≥99 %, Sigma Aldrich), heptanal (95 %, Sigma Aldrich) and syngas ($CO:H_2 = 1:1$, LLC "PGS Service", Russia) were used as received. $Rh(acac)(CO)_2$ was synthesized according to the procedure published in [25] from $RhCl_3{*}4H_2O$ («Aurat» LLC). The solvents (toluene, THF, and *n*-hexane) were dried according to standard procedures. *Iso*-propyl alcohol (*i*PrOH, pure, LLC "Ekos-1", Russia) was used as received.

In a typical catalytic experiment, $Rh(acac)(CO)_2$, solvents, amine, and substrate were loaded into a quartz test-tube equipped with a stir bar. For Rh precursor weighting, the balance with accuracy = ± 0.1 mg were used. In catalytic experiments with 1 mg $Rh(acac)(CO)_2$ loading, we previously prepared solution of 10 mg $Rh(acac)(CO)_2$ in 10 mL of toluene, and then transferred 1 mL aliquot into the test-tube. The test-tube was covered with perforated foil and put in a stainless steel autoclave (50 mL). The autoclave was sealed, purged with syngas and pressurizes with syngas to 3.0 MPa. The mixture was stirred (700 rpm) at 90℃ for 1 h, then the autoclave was cooled down, depressurized and opened. The internal standard (*n*-dodecane) was added to the test-tube, the mixture was stirred for 30 s and was analyzed by gas–liquid chromatography on a Chromos GS-1000 chromatograph ("Chromos Engineering" LLC, Russia) equipped with a flame ionization detector and a 50-m-long capillary column coated with the DB-5 phase using temperature programming of 60–230 °C and helium as a carrier gas. Catalytic experiments were performed three times, and then the average value and standard deviation were calculated.

2.2. X-ray absorption measurements

Rh K-edge X-ray absorption spectra (XAS) were measured at the beamline "Structural Materials Science" [26] using the equipment of Kurchatov Synchrotron Radiation Source (Moscow, Russia). We modified the transmission cell for *in situ* XAS studies reported in [27,28]. The cylindrical stainless steel autoclave with two coaxial holes for the X-ray beam was further equipped with a furnace with coaxial holes of a bigger diameter (Fig. 2).

The external heater was found to be preferential over the integrated one within steel body due to the better temperature control and closer contact with a magnetic stirrer. The reagents $(Rh(acac)(CO)_2$ 10 mg, amine 0.014 mol, toluene/*i*PrOH 1:2 vol 5-x mL (x is volume of a ligand), were loaded into a Teflon vessel. The latter was tightly attached to the inner wall of the autoclave. For each reaction mixture, the spectra were firstly recorded after stirring under atmospheric conditions. Then, syngas (3.0 MPa) was introduced into the autoclave, with subsequent heating to 90℃. High stirring speed (700 rpm) was applied during first 5 min and then it was decreased to 200 rpm when *in situ* spectra were recorded. The storage ring with an electron beam energy of 2.5 GeV and a current of 80–100 mA was used as the source of radiation. All spectra were collected in the transmission mode using a Si(220) channel-cut monochromator. Three ionization chambers monitored the intensity of the X-ray beam before and after the sample, and after the reference sample for energy calibration.

A multi-shell Fourier approach was applied for EXAFS data analysis.

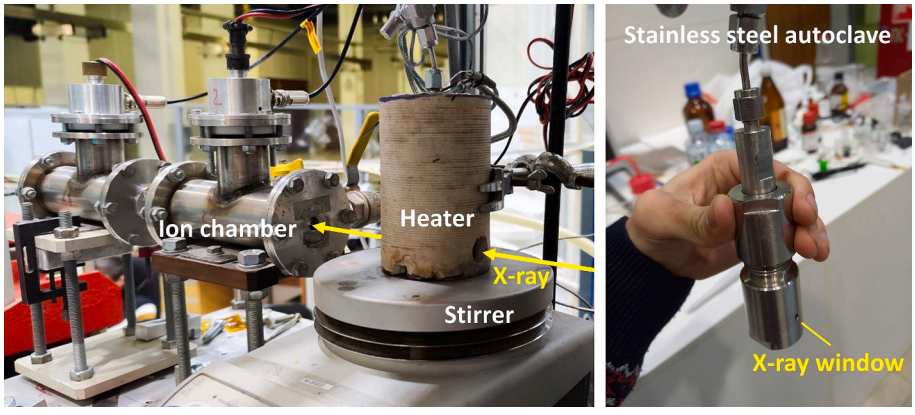

Fig. 2. Experimental setup for *in situ* synchrotron XAS measurements. *The first ionization chamber is installed before stainless steel autoclave and not shown in the figure. The autoclave without heater is shown separately in the right panel and has two coaxial holes for transmission measurements.*

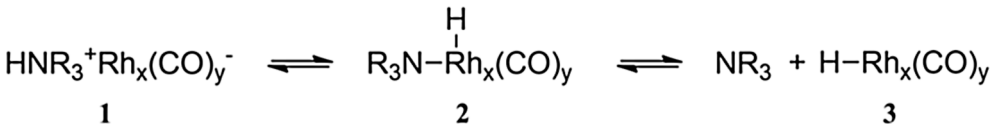

Background subtraction, normalization, energy alignment, and extraction of χ(k) oscillatory function were performed in the Athena program of the Demeter package [29]. Further analysis in Artemis program included calculation of theoretical amplitudes and phases by the FEFF6 code [30] and fitting in the R-space of the Fourier-transformed data k^2-weighted χ(k) applying Δk Hanning window from 3 to 11.0 $Å^{-1}$ with the width of the window slope dk = 1 $Å^{-1}$. The range in R-space for fit of amine-based systems at ambient conditions was limited to the first coordination shell only, while for amine-free and all the samples under reaction conditions it was extended up to 3 Å since multiple scattering from Rh-CO and single scattering from Rh-Rh were also important. The fitting parameters included distances and coordination numbers from Rh to linear CO, nondistinguishable C/O/N atoms in the ligands and Rh. When linear CO was included in the fit the single scattering from Rh-O and multiple scattering from Rh-C-O were considered beyond Rh-C shortest path. The Debye-Waller factors (σ^2), zero energy shift (ΔE_0) and the value of passive electron reduction factor (S_0^2) were obtained by fitting reference $Rh(acac)(CO)_2$ sample and then fixed whenever possible for all other fits. For each sample several fits were performed starting from different initial conditions and those providing similar nonstructural parameters with the all other fitted spectra were left in the final report. Finally, we ensured that number of parameters for each fit didn't exceed the number of independent points N_{ind}, defined as

$$N_{ind} = (2\Delta r \Delta k/\pi) + 1 \quad (1)$$

where Δk – is the region of EXAFS spectrum in k-space used for the Fourier analysis, Δr – is the region in R-space for the Fourier filtration.

2.3. Computational details

Geometry optimization and electronic structure calculations were performed within density functional theory (DFT) in AMS-2022 program package [31]. A benchmark test was carried out for several GGA, hybrid and *meta*-GGA exchange correlation functionals. Meta-GGA TPSS [32] with DFT-D3 [33] dispersion corrections and Becke–Johnson damping [34] (D3(BJ)) was chosen as a good compromise of accuracy and computational performance. The triple-ζ basis set with one polarization function (TZP) was used for geometry optimization and single point energy calculations.

3. Results and discussion

It is known from the previous studies that Rh/NR_3 systems have sufficient activity in hydrogenation of aldehydes only in presence of CO [21,35], implying that CO must be included into the species active for this reaction. Also, Rh clusters were detected in catalytic solutions [24,36,37]. The equilibrium existing under syngas pressure is described by the following scheme [24]:

Species **2** is believed to be active in aldehyde hydrogenation; hydroformylation is presumably catalyzed by both species **2** and **3**. The hydrogenation stage is selective to C = O double bonds over C = C: thus, cynnamic alcohol can be obtained by hydrogenation of cynnamal in a Rh/NR_3 system with > 80 % selectivity [38]. In the absence of CO, C = C double bonds are readily hydrogenated [21,38].

In 2021, Rosler et al. [36] published their thorough study, which was mainly focused on the effect of the amine ligand properties on the yield of alcohols in reductive hydroformylation. They examined experimentally more than ten different ligands and showed that both basicity and steric properties of the ligand are important for an efficient production of alcohols. The values of *p*Ka 8.5–11.5 and a cone angle 135-155° were found to be the most suitable. However, it was still not clear to what a degree each stage of the tandem process was influenced by those features. To uncover the influence of ligands on each stage of the reaction we performed both of them with various ligands separately. The structures of the ligands studied in our work are shown in Fig. 3.

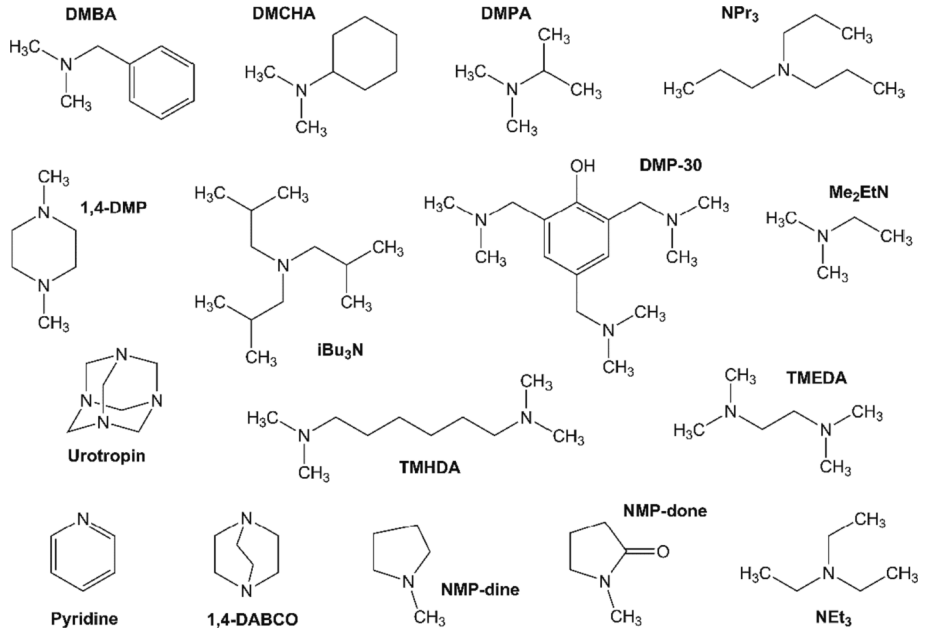

Fig. 3. The structures of the N-ligands used.

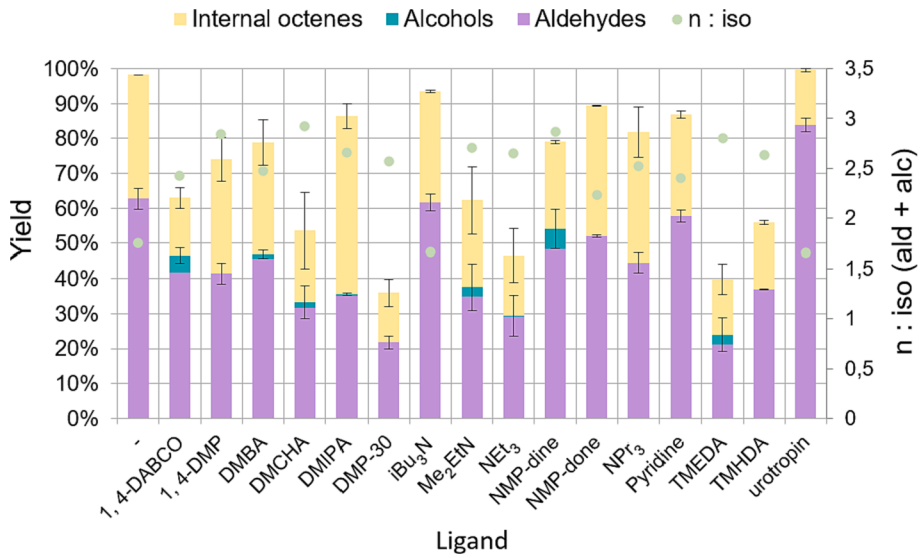

Fig. 4. Hydroformylation of hexene-1 with various N-ligands. *Conditions: $Rh(acac)(CO)_2$ 1 mg ($3.9 * 10^{-6}$ mol), hexene-1 0.5 mL ($4.0 * 10^{-3}$ mol), ligand 1.8 mmol (N atom), toluene 4-x mL (x is volume of a ligand), 90°C, 4.5 MPa (CO: H_2 = 1:1), 1.5 h.*

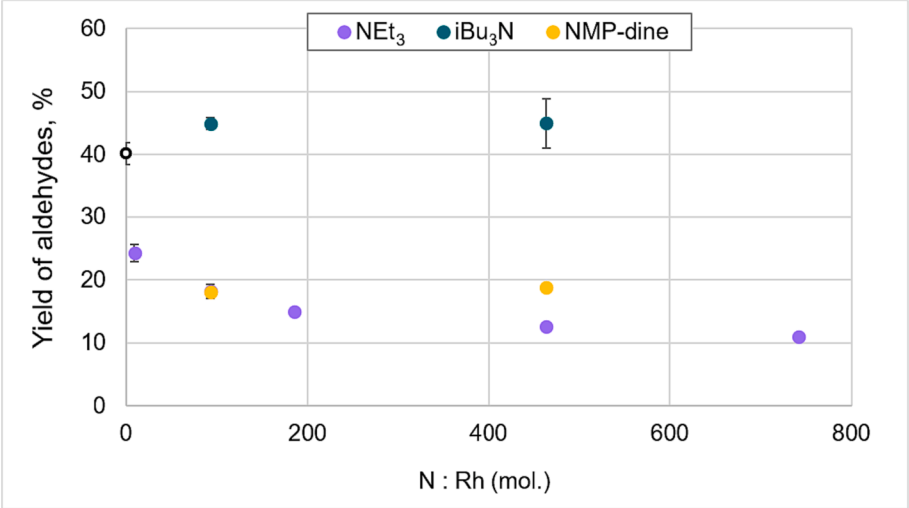

Fig. 5. Hydroformylation of hexene-1 at diffefent concentrations of amines. *Conditions: $Rh(acac)(CO)_2$ 1 mg ($3.9 * 10^{-6}$ mol), hexene-1 0.4 mL ($3.2 * 10^{-3}$ mol), toluene 4-x (x is volume of a ligand), 90°C, 4.5 MPa (CO:H_2 = 1:1), 1 h.*

3.1. Influence of amine ligands on the hydroformylation stage

In the tandem process hydrogenation and hydroformylation processes coexist and the latter produces aldehydes for the subsequent conversion into alcohols. In hydroformylation experiments we did not prioritize high yields of alcohols, but rather picked the conditions to keep the summed yield of oxygenates on the levels appropriate for the comparison between different systems (20–60 %) (Fig. 4).

Although in the work [10] the authors claimed that the amine addition has a positive effect on hydroformylation rate, our data confirm the opposite: under the studied conditions most amines decrease the hydroformylation yield. Triisobutylamine had no effect either on activity or on regioselectivity of the system in hydroformylation, which may lead to the conclusion that its interaction with Rh under the conditions studied is rather weak. Pyridine was found to increase *n: iso* ratio and slightly reduce the rate of double bond isomerization. The only amine that significantly promoted hydroformylation was urotropin. As its concentration was lower than that of others due to its poorer solubility in toluene, we performed a series of experiments with other ligands in various concentrations to find out if there is some optimal N-ligand content (Fig. 5).

The time of the reaction in this series was shorter, so no alcohol formation was observed in these experiments. Even at as low concentrations as 0.08 M (0.005 mL, N: Rh = 9: 1), triethylamine reduces the rate of hexene-1 hydroformylation. It drastically falls till N: Rh ratio of 100–200: 1 (0.05 – 0.1 mL) and then reduces much slower. This "remaining" activity is probably what makes possible the tandem process at high amino concentrations, which are preferable for the second hydrogenation stage. In this series, NMP-dine also significantly inhibited hydroformylation for the whole range of concentrations. The presence of *i*Bu_3N had a little impact on hydroformylation rate, interestingly, rather a positive one. So, at least under the studied conditions, tertiary amines, that are effective hydrogenation promoters, reduce the activity of Rh complexes in hydroformylation. The phenomenon of higher aldehyde yields with urotropin needs more studies to be explained. Although in the series presented in Fig. 4 Rh/urotropin system provided no alcohol yields either in tandem process or in aldehyde hydrogenation (Fig. 6), according to the additional experiments, it is capable of reductive

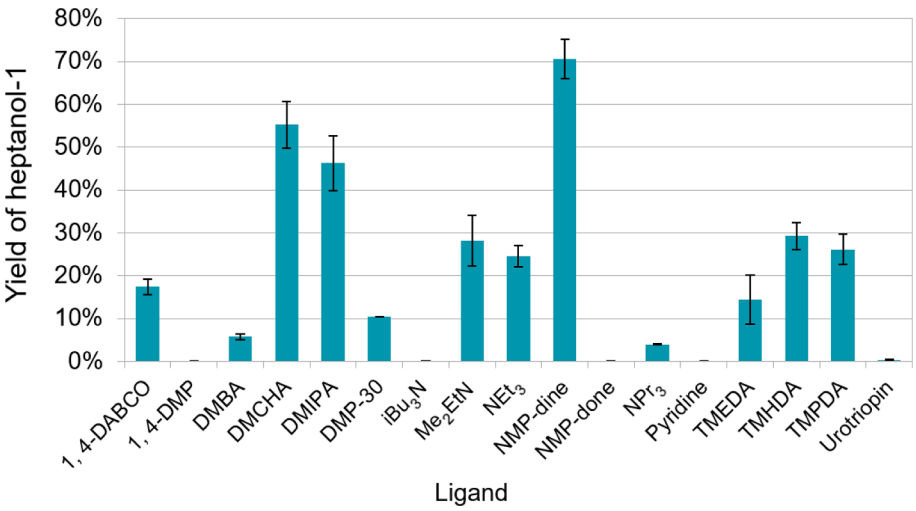

Fig. 6. Hydrogenation of heptanal with various N-ligands under syngas pressure. *Conditions: Rh(acac)(CO)$_2$ 1 mg (3.9 * 10^{-6} mol), heptanal 0.47 mL (3.3 * 10^{-3} mol), ligand 1.8 mmol (N atom), toluene 4-x mL (x is volume of a ligand), 90°C, 3 MPa (CO: H$_2$ = 1:1), 1.5 h.*

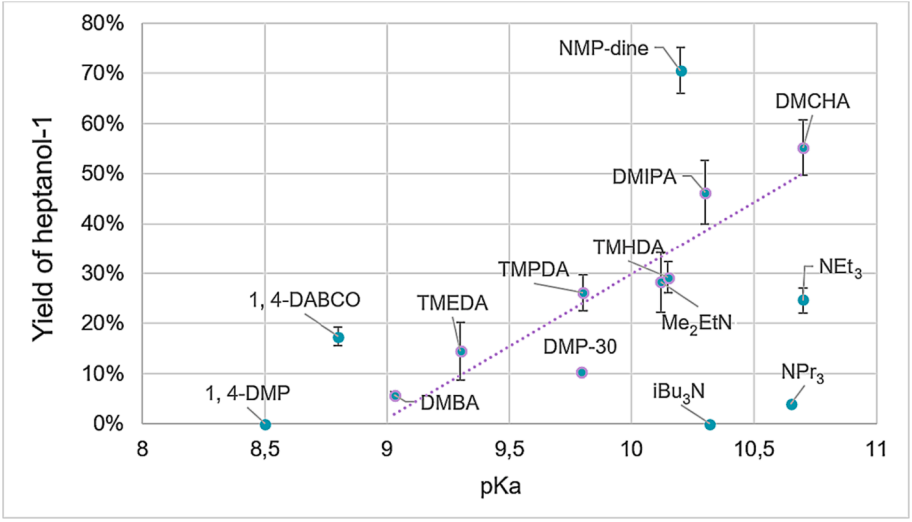

Fig. 7. The yield of hexanol-1 vs pKa of the amine ligands in the hydrogenation reaction. *Conditions: Rh(acac)(CO)$_2$ 1 mg (3.9 * 10^{-6} mol), heptanal 0.47 mL (3.3 * 10^{-3} mol), ligand 1.8 mmol (N atom), toluene 4-x mL (x is volume of a ligand), 90°C, 3 MPa (CO: H$_2$ = 1:1), 1.5 h. For bidentate amines, pKa$_1$ is given.*

hydroformylation at higher temperature (100-120°C) and prolonged reaction time (3 h).

3.2. Influence of amine ligands on aldehyde hydrogenation

To address the second stage of the tandem process, the ligands were tested in a separate reaction of aldehyde hydrogenation (Fig. 6). The reactions were conducted under lower pressure than hydroformylation (3 MPa vs 4.5 MPa) to obtain a proper differentiation in alcohol yields within same reaction time.

The systems with pyridine and N-methylpyrrolidone, non-amine type ligands, provide no hydrogenation. With urotropin, the yield of heptanol-1 is almost 0 % as well, however, its decreased concentration caused by low solubility might play a decisive role, as this reaction is strongly dependent on amine concentration [24]. For other amine ligands we observed a correlation between their bacisity and hydrogenation activity (Fig. 7).

None of the ligands with *p*Ka < 9.5 provided high yields of the hydrogenation reaction. If only R-NMe$_2$ ligands are taken into account (rounded with purple), the dependence is close to linear. However, we also observed an effect of steric properties of the ligand. In the row NEt$_3$ – NPr$_3$ – *i*Bu$_3$N hydrogenation activity drops with an increase in the alkyl substituent length. Interestingly, for tetramethylamines (TMEDA, TMPDA, TMHDA) the tendency is opposite: Rh/TMHDA system was the most active of three. Both lines follow the general trend of increasing the activity with the growth of *p*Ka, but for NEt$_3$, NPr$_3$ and *i*Bu$_3$N the yields are lower than it might be expected from their basicities. This is most probably caused by the steric hindrance of three substituents ≥ C$_2$.

Basicity seems to be less important for the activity in hydroformylation of hexene-1 (fig. S.1). We did not observe a pronounced effect of *p*Ka on the total oxygenate yields. It is worthwhile mentioning that in NEt$_3$ – NPr$_3$ – *i*Bu$_3$N row the last ligand provides the highest yield in hydroformylation. Together with the hydrogenation data, it may suggest that, due to steric hindrance, Rh-N interaction decreases in this row.

Interesting data was obtained with cyclic amines. The highest yields of alcohols in both series were achieved with N-methylpyrrolidine (NMP-dine). In addition, it causes a smaller decrease in hydroformylation rate compared to DMCHA and DMIPA, which also provide good hydrogenation yields. However, its bidentate six-membered analogue 1,4-DMP is totally ineffective in aldehyde hydrogenation and decreases hydroformylation by 20 %. This probably means that it does

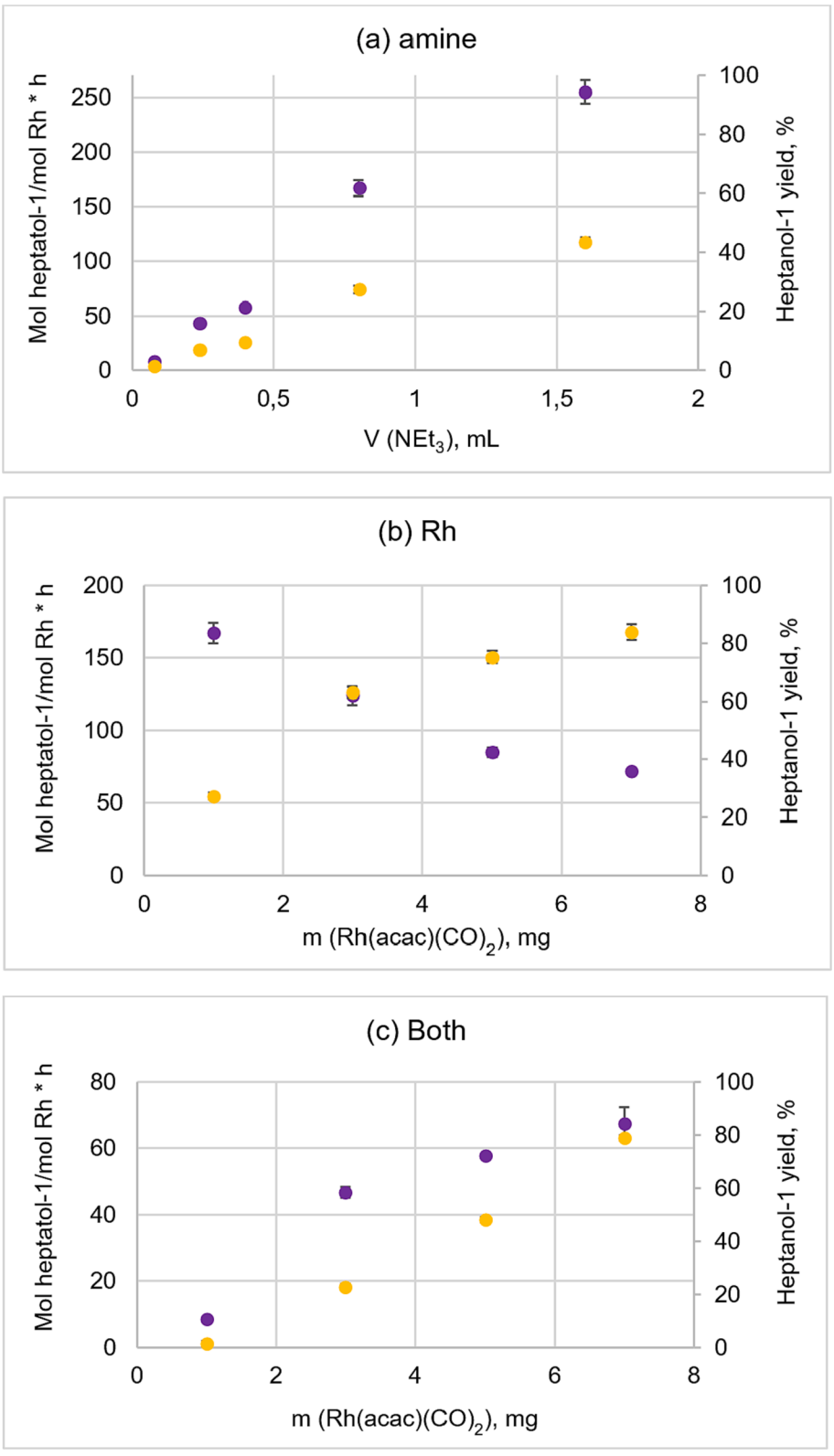

Fig. 8. Effect of Rh and amine concentration on the activity in heptanal hydrogenation. Activity per Rh atom, Yield of heptanol-1. *Conditions: heptanal 0.3 mL (2.1 * 10^{-3} mol), toluene 3-x mL (x is volume NEt_3), iPrOH 2 mL, 90C, 3 MPa (CO: H_2 = 1:1), 1 h; a) $Rh(acac)(CO)_2$ 1 mg (3.9 * 10^{-6} mol); b) NEt_3 0.8 mL c) N: Rh = 150: 1.*

coordinate with Rh under reaction conditions, but being a weaker base, does not donate enough electron density on Rh center for successful hydrogenation. More basic 1,4-DABCO appears to be quite effective specifically in the tandem reaction: while with many other ligands aldehyde hydrogenation rate is higher, the yield of alcohols in reductive hydroformylation with 1,4-DABCO is second only to the most active Rh/NMP-dine system.

Another process affected by amines is the equilibrium between mononuclear Rh complexes and metallic clusters. Several times it was reported [24,36,37] that in Rh/NR_3 systems Rh clusters are formed

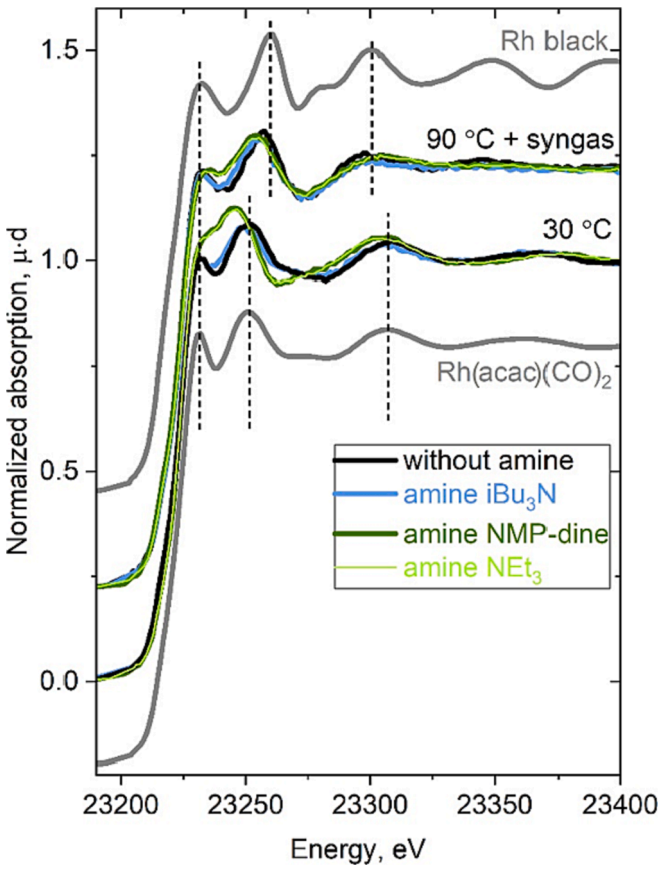

Fig. 9. Rh K-edge XANES spectra for the catalytic systems under ambient (30 °C, air) and reactive (90℃, 3.0 MPa syngas) conditions.

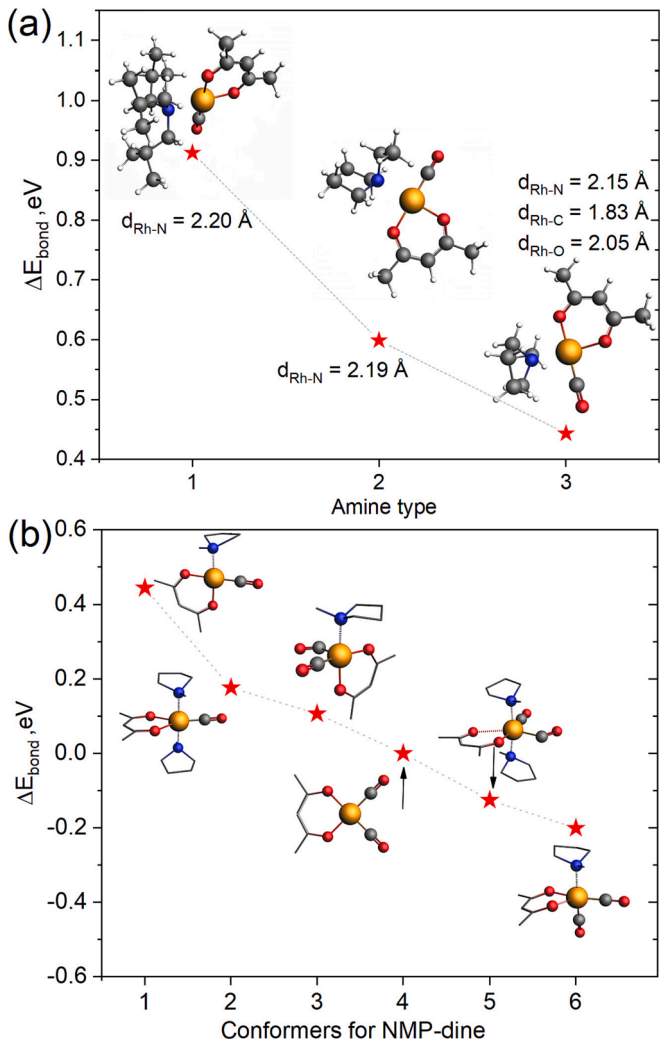

Fig. 10. (a) Bonding energies of Rh(acac)(CO)(amine) with amine equal *i*Bu_3N, NEt_3, NMP-dine with respect to the reference structure Rh(acac)$(CO)_2$. (b) Possible conformers of Rh(acac)$(CO)_x(amine)_y$ complexes (1–6) arranged in decreasing order of total bonding energy.

under syngas pressure. However, it was not quite clear if the clusters catalyze hydrogenation, or clusterization is a side process resulting from insufficient Rh-L interaction. To obtain new insights into this question, we studied heptanal hydrogenation at different Rh and amine concentrations. In Fig. 8 a-c, the three series of experiments are shown: in series (a) Rh concentration was fixed and only NEt_3 quantity was varied, in (b), Rh loading was varied at constant amine volume, and in (c) we varied both Rh and NEt_3 quantities fixing Rh:N ratio.

The experiments were performed in toluene/*i*PrOH media to prevent deposition of Rh at higher metal concentrations, which we detected if only toluene was used as a solvent. We suggest the residue to be an ionic complex with a structure close to $[NEt_3H]^+[Rh_x(CO)_y]^-$. The formation of complexes of this type was assumed by many preceding works [15,24,36,37] and even was exploited by Monflier's group for multiple use of Rh secured by their high affinity to acetone [13]. In this series, we chose to add *i*PrOH to have a control over Rh concentration in the solution in order to study its effect.

The order by aldehyde in Rh/NR_3-catalyzed hydrogenation was previously reported to be zero [35], which makes it possible to compare the rates of the reaction at various substrate conversions. In all three series, the yield of heptanol-1 increased with the addition of Rh or/and amine, but the activity per Rh atom demonstrated another pattern: it increased if NEt_3 was added and decreased with the growth of Rh concentration at constant amine loading. One of the most probable explanation is that the formation of Rh clusters reduces the productivity of Rh centers in this process, so they are either inactive or less active than mononuclear Rh species (or clusters with lower nuclearity are more active compared to high-nuclear clusters) [39]. The order by Rh calculated from the data in Fig. 8-b is about 0.6 (±0.1).

Within this hypothesis, the addition of amine may prevent clusterization by bonding with Rh, or promote the formation of smaller clusters, so the activity per Rh atom increases with amine concentration in series (a) and (c). This role of amine can be considered as an additional to its immediate influence on Rh through the electron density donation, although these two aspects are obviously related. The order by NEt_3 from series (a) can be estimated as 1.3(±0.1).

3.3. *In situ* XAS measurements and quantitative interpretation

As in the systems of this type many dynamic equilibria co-exist under the reaction conditions, for the understanding of their functioning, they should be studied directly in catalytic solutions under the conditions as close to the reaction ones as possible. This limits the range of instrumental methods to sensitive, selective, and applicable to liquid probes. The Rh/NR_3 catalytic system was previously studied by NMR and IR spectroscopies, including *in situ* experiments under elevated syngas pressure [36,37]. Here we applied X-ray absorption spectroscopy to investigate the changes taking place in Rh coordination sphere during its interaction with amines and syngas. Fig. 2 shows experimental setup for *in situ* measurements. The stainless-steel autoclave has Teflon vessel with magnetic stirrer inside. Two small holes were drilled in the steel case of autoclave for transmission measurements. 2 mm thick Teflon walls and small size of holes were able to withstand up to 6 MPa syngas pressure and 90 ℃ heating during reaction without additional

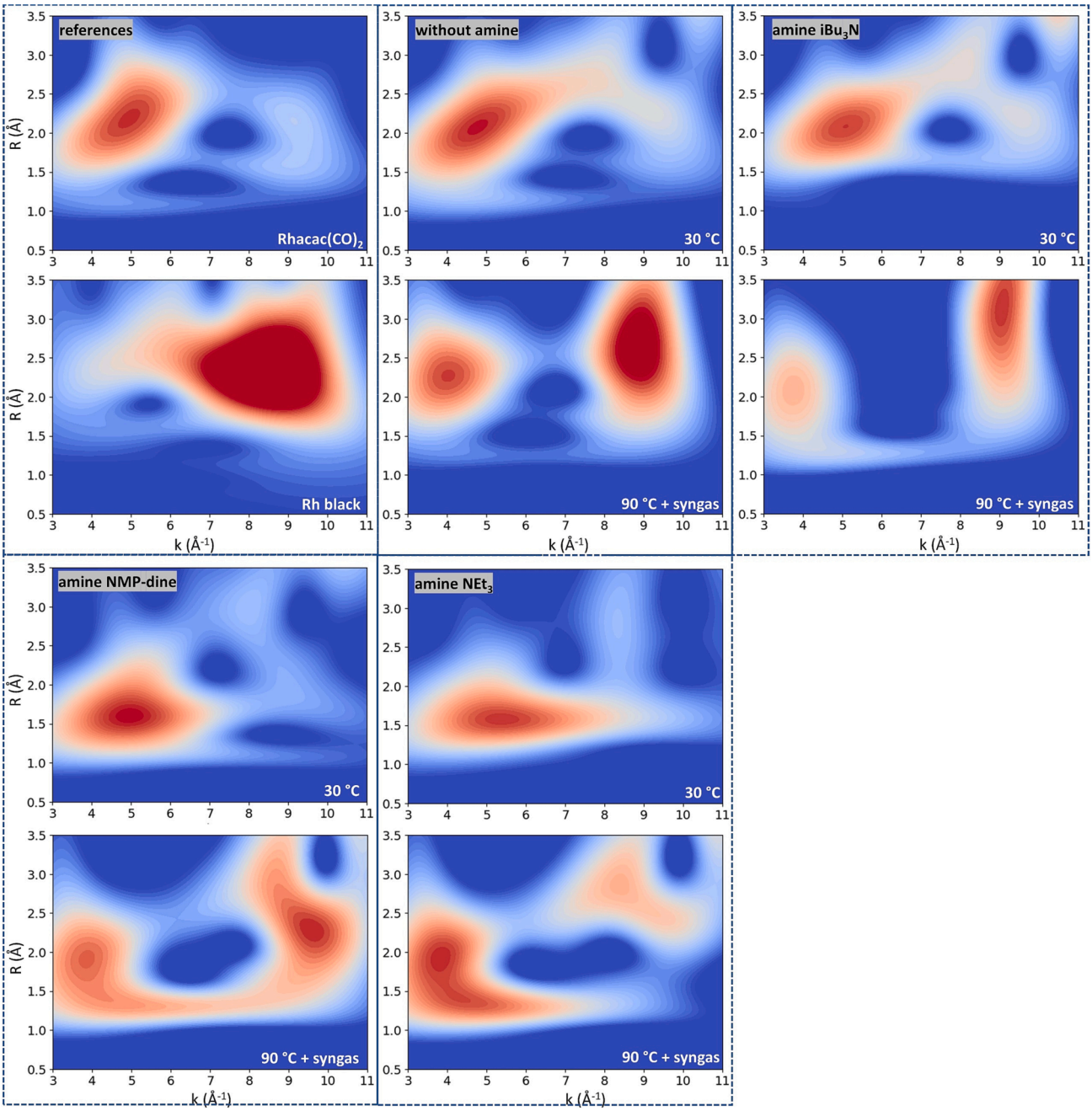

Fig. 11. Wavelet transform maps for studied catalytic systems at ambient conditions and under syngas at 3.0 MPa and 90°C. *The region $k = 8...10$ Å^{-1} and $R = 2...3$ Å is indicative for Rh-Rh scattering.*

mechanical protection. The measurements were performed under conditions with high concentration of active species allowing to elucidate the role of three different amines in the catalytic cycle. Therefore, we used toluene/*i*PrOH solution to prevent Rh deposition. However, without an amine we observed the formation of the red-color Rh carbonyl crystals whose XAS spectrum was similar to the one from reaction liquid under *in situ* conditions.

Fig. 9 shows variation of the Rh K-edge XAS spectra upon addition of the amines in the reaction mixture at ambient conditions – room temperature and without addition of syngas. The intensity of the white line in the region 23230–23250 eV increases slightly after adding *i*Bu_3N amine and then significant changes occur in the system with NEt_3 and NMP-dine amines. Narrow and intense white line in XAS spectra indicates higher coordination number of metal center and corresponds to penta- or *hexa*-coordinated Rh-amine complexes. Therefore observed spectral changes highlight the larger structural reorganization in the catalytic systems containing NEt_3 and NMP-dine ligands compared to *i*Bu_3N. DFT/TPSS-D3(BJ) calculations further confirm lower energy of the resulting complexes coordinated by NMP-dine and NEt_3 ligands. Fig. 10-a demonstrates classical ligand exchange process when amine substitutes carbonyl as was shown experimentally for tertiary phosphines [40]. All considered species are higher in energy with respect to the original $Rh(acac)(CO)_2$ complex since the Rh-CO bond is stronger. However due to high concentration of amines such geometries may be accessed thermodynamically. Steric effects increase the energy of complex coordinated by *i*Bu_3N, while complex with small NMP-dine ligand is the most stable with respect to the value of bonding energy. The bond length to amine varies from 2.15 to 2.25 Å for NMP-dine and NEt_3 and being slightly elongated for *i*Bu_3N.

Based on the bonding energy calculations we propose several

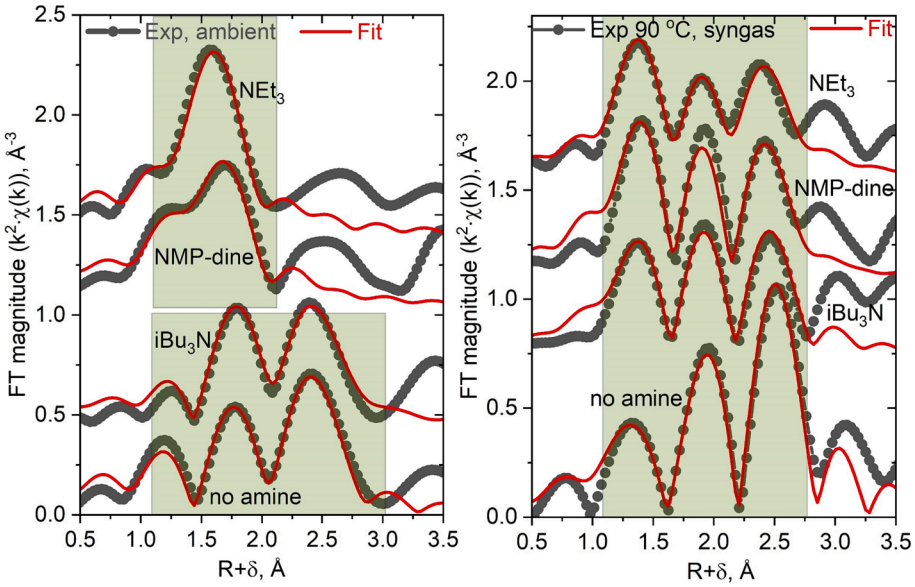

Fig. 12. Magnitude of the k^2-weighted Fourier transform experimental χ(k) data in the range 3…11 A^{-1} compared to the theoretical fits. *Green rectangles indicate the region in the R-space used for fit. Each panel contains four experimental spectra for system without amine (bottom), with iBu₃N, NMP-dine, NEt₃ (top) amines measured at ambient (left panel) and reaction (right panel) conditions.* (For interpretation of the references to color in this figure legend, the reader is referred to the web version of this article.)

candidates that can coexist in the equilibrium (Fig. 10-b). The lowest energy was observed for complexes with distorted square pyramidal or trigonal bipyramidal coordination. To achieve such configuration two bonds Rh-O to acac ligand become unequal, one being elongated up to 2.4 Å from its initial value 2.1 Å. Predicted lower energies for complexes with amines along with observed variations in XAS prove the coordination of Rh with nitrogen through changing the square planar geometry of the complex to 5- and 6-coordinated species.

The differentiation between solutions with three different amines was also observed in XAS spectra at reactive conditions: 90°C temperature and 3.0 MPa pressure of syngas. The spectrum of catalytic system at these conditions without addition of amines (black curve) contains signatures from both carbonyl ligands and metallic Rh suggesting presence of Rh carbonyl clusters. Temperature and concentration of dissolved hydrogen and carbonyl molecules shifts the equilibrium between metal carbonyls of different nuclearity [41]. Amines further affect this equilibrium decreasing the concentration of metallic clusters. Addition of *i*Bu_3N amine has prominent but small effect on Rh K-edge XANES spectrum (blue curve) while NEt_3 and NMP-dine under reaction conditions induce larger changes in the spectra. We proceed with qualitative and quantitative EXAFS analysis to address further details in the local coordination of Rh.

The wavelet transform of the Rh K absorption edges allows a qualitative description of the rhodium coordination sphere. It provides a two-dimensional representation of the EXAFS spectrum, thus characterizing the signal simultaneously in k- and R-space. This method is based on the fact that the contributions to the photoelectron scattering paths arising from ligand atoms with different Z number around absorbing atom, are localized in different regions of the k-space. The signals from heavier atoms tend to be localized at higher wavenumbers. We have carried out the EXAFS wavelet analysis for the catalytic system at ambient and reaction conditions compared to metallic rhodium and $Rh(acac)(CO)_2$ standards. The WT-maps are shown in Fig. 11.

The wavelet-transform maps are sensitive to the Rh-Rh scattering at wavenumbers region k = 8…10 $Å^{-1}$. The WT spectrum of metallic rhodium and sample at reactive conditions without amine contains intense feature in this k-region for distances near R ~ 2.5 Å (phase uncorrected value). The amplitude of the signal in this region is highest for the sample in amine-free system, while after addition of amines the intensity was reduced. Such behavior suggests presence of Rh clusters with Rh-Rh bonds in the reaction mixture without amines. The addition of amines inhibits the formation of clusters.

Quantitative fit of the spectra acquired under reaction conditions is nontrivial due to their heterogeneity. Various isomers of the complexes

Table 1
Structural parameters obtained from EXAFS fit for system under ambient conditions. Single scattering paths from C in acac and O in CO at 2.9 A and multiple scattering paths from CO at 2.9 A were included in the fit for *i*Bu_3N and complex without amine but omitted in the table.

Sample	Coordination sphere	Coordination number	Distance, Å	DW factor	E_0, eV	S_0^2	R factor
$Rh(acac)(CO)_2$	C(CO)	2.1	1.86 (1.85 XRD)	0.0015	5.0	1.2	0.02
	O(acac)	2.1	2.04 (2.04 XRD)	0.0020			
$Rh(acac)(CO)_2$, NMP-dine	C(CO)	1.5	1.89	0.0015	6.0	1.2	0.02
	C/O/N	1.9	2.00	0.002			
	C/O/N	2.3	2.13	0.002			
$Rh(acac)(CO)_2$, NEt_3	C(CO)	1.1	1.87	0.0015	6.0	1.2	0.02
	C/O/N	2.8	2.02	0.002			
	C/O/N	1.3	2.16	0.002			
$Rh(acac)(CO)_2$, *i*Bu_3N	C(CO)	1.7	1.88	0.0015	6.0	1.2	0.01
	C/O/N	1.5	2.03	0.002			
	C/O/N	1.3	2.14	0.002			

Table 2
Structural parameters obtained from EXAFS fit under reaction conditions (3.0 MPa syngas, 90°C). Multiple scattering paths from CO at 2.9 A were included in the fit but omitted in the table for clarity.

Sample	Coordination sphere	Coordination number	Distance	DW factor	E_0	S_0^2	R factor
$Rh(acac)(CO)_2$	C(CO)	2.0	1.90	0.0015	4	1.2	0.02
	C/O	1.0	2.09	0.0020			
	Rh	2.7	2.74	0.005			
$Rh(acac)(CO)_2$, NMP-dine	C(CO)	0.9	1.90	0.0015	5	1.2	0.04
	C/O/N	2	1.96	0.0020			
	C/O/N	1.6	2.14	0.0020			
	Rh	1.0	2.70	0.005			
$Rh(acac)(CO)_2$, NEt_3	C(CO)	1.2	1.88	0.0015	3	1.2	0.01
	C/O/N	1.3	1.95	0.0025			
	C/O/N	1.1	2.17	0.0025			
	Rh	0.7	2.70	0.005			
$Rh(acac)(CO)_2$ $i$$Bu_3N$	C(CO)	1.0	1.89	0.0015	3	1.2	0.02
	C/O/N	1.3	1.97	0.002			
	C/O/N	1.2	2.14	0.002			
	Rh	1.6	2.74	0.005			

Table 3
Results of catalytic experiments under the conditions applied for XAS measurements.

Ligand	Hydrogenation of heptanal [a]	Hydroformylation of hexene-1 [b]
–	alcohol, 0.5 %	aldehydes, 38 %
$i$$Bu_3N$	alcohol, 4 %	aldehydes, 25 %
NEt_3	alcohol, 97 %	aldehydes, 10 % alcohols, 7 %

Conditions: 10 mL autoclave, Rh(acac)(CO)2 10 mg ($3.9 * 10^{-5}$ mol), amine 0.014 mol, toluene/iPrOH 1:2 vol 5-x mL (x is volume of a ligand), 90°C, 3.0 MPa (CO: H2 = 1:1); 1 h; a) heptanal 0.5 mL ($3.5 * 10^{-3}$ mol), b) hexene-1 0.5 mL ($4.0 * 10^{-3}$ mol).

may be present in the solution under equilibrium conditions. Moreover the distances in the first coordination shell of Rh may differ significantly within a single complex. Coexistence of several close distances follows from different bond types to carbonyl, acac, amine and Rh-Rh ligands and is confirmed by DFT geometry optimization (see fig. S.3).

One way to reduce the ambiguities in the fit is the use the simplest allowable model and fixing some of the parameters, such as Debye-Waller factors, S_0^2 by using references. When several good fits were found with similar R-factors the preference was given to the ones with similar values of the energy shift E_0. The results of the quantitative EXAFS analysis are shown in Fig. 12 and Tables 1-2.

The EXAFS data of the $Rh(acac)(CO)_2$ solution in toluene and iPrOH under atmospheric conditions in general corresponds to the crystallographic structure of the complex with two Rh – CO and two Rh – O bonds. The overall coordination number of Rh in the first coordination sphere increases upon addition of amines reaching 5.8 in NMP-dine. The EXAFS spectrum has no sensitivity to the type of light atoms C, O, or N. However, one can speculate that NMP-dine binds to Rh as the additional ligand, causing the rearrangement of the other ligands. The coexistence of fraction of species with substitution of one CO to NMP-dine is also possible [40]. The changes were also observed with other amines – NEt_3 and $i$$Bu_3N$. Obviously, even $i$$Bu_3N$, the impact of which on the catalytic performance is the weakest of the three, provides some divergences. They were the smallest but still prominent both in XANES and EXAFS regions. However, the total Rh coordination number for catalytic system with $i$$Bu_3N$ amine was 4.5, and the coordination number for linearly bonded CO was the largest, which is close to the amine-free system.

After heating under syngas pressure, we observed the contribution from Rh-Rh scattering at 2.7…2.74 Å, that is larger than 2.69 Å in metal. We can thus prioritize the formation of small clusters since Rh-Rh scattering was also accompanied by two different types of light atoms at 1.90 and 2.09 Å that can be referred to the terminal and bonding CO ligands in carbonyl clusters (see [42] and fig. S3 in SI). In the systems with amines, a good fit required addition of third light atom at distance ca 2.15 Å. Additionally the number of Rh-Rh bonds decreased compared to the amine-free experiment. Of the three amines, the largest Rh-Rh coordination number equal to 1.6 was obtained for $i$$Bu_3N$, the least

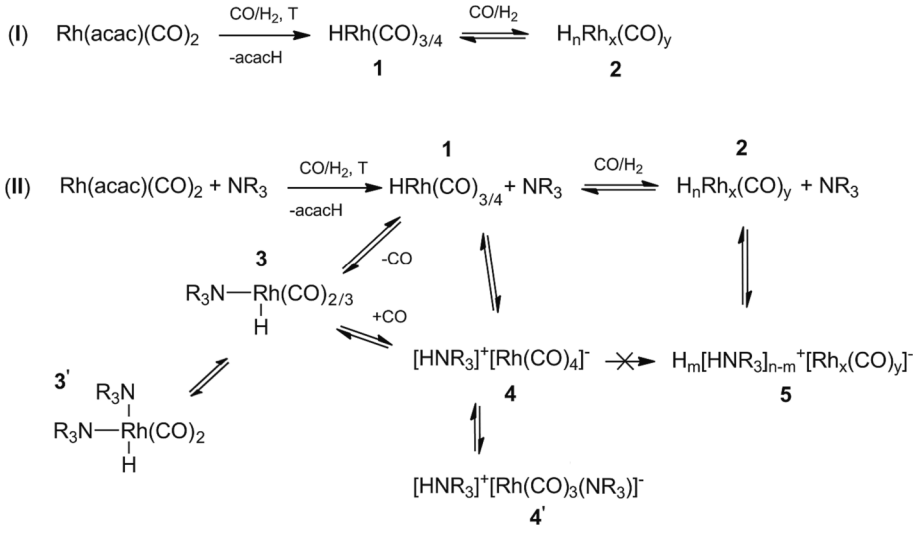

Fig. 13. Possible transformations of Rh species under the reaction conditions.

effective ligand for aldehyde hydrogenation, while for NMP-dine and NEt_3 it was ≤ 1.

Under the reaction conditions of heptanal hydrogenation in amine-free and NEt_3-containing systems, we found similar behavior of Rh-Rh coordination number being about two times lower with NEt_3. The experiments were carried on about 1 h; the GLC analysis of the resulting mixtures provided 0.5 % and 97 % yields of heptanol-1 without an amine and with NEt_3, respectively (Table 3). Later, we performed the hydrogenation test with iBu_3N under approximately analogous conditions to ensure that with high Rh concentrations and toluene/*i*PrOH medium the effect of ligand structure remains similar. The yield of alcohol in this case was 4 %. Therefore we found spectroscopic evidence of decreasing aldehyde hydrogenation effectivity along with increasing Rh-Rh coordination number. The simplest explanation is the lower activity of the Rh carbonyl clusters in this reaction.

Rh clusters were shown to be active in hydroformylation under low pressures without a total decomposition [43], although the effectiveness of Rh centers use is expectedly lower in this case. The catalytic system prepared for *in situ* XAS experiments demonstrates similar pattern obtained in Fig. 4 for significantly smaller catalyst concentration.

To sum up, from the data obtained it is reasonable to suggest that tertiary amines, at least in high concentrations, inhibit Rh clusterization, forming mononuclear/low nuclear complexes with Rh-N coordination, which are active in aldehyde hydrogenation, but inactive (or slightly active) in hydroformylation of olefins. Too sterically hindered ligands, such as triisobutylamine, have a smaller impact on Rh coordination sphere, presumably not forming enough N-Rh bonds, and demonstrate results close to amine-free catalyst in both hydroformylation and hydrogenation. They also reduce the Rh-Rh coordination number, but this does not affect catalytic behavior significantly, since for aldehyde hydrogenation Rh-N bonds are necessary, and in hydroformylation the Rh clusters are satisfactorily active. The complimentary picture is observed under ambient conditions. NMP-dine and NEt_3 amines, which are effective in aldehyde hydrogenation form coordination complexes with the Rh centers, while the effect of *i*Bu_3N addition is much less pronounced.

3.4. Possible transformations of Rh species under the reaction conditions

The possible scheme of the transformations of Rh complexes under the reaction conditions in absence (**I**) and presence (**II**) of amine is shown in Fig. 13. For amine-free system, polynuclear hydridocarbonyls (**2**) are formed. Polynuclear Rh complexes were previously proved to be stable and active in hydroformylation under mild conditions (3.4 MPa, 125℃) [43]. So, although clusterization most probably decreases hydroformylation TOF (per Rh atom), both species (**1**) and (**2**) contribute to hydroformylation.

The addition of basic amines results in the formation of species (**4**), preventing Rh clusterization. It is formed independently of steric properties of the amine. On the other hand, complex (**3**) with the direct bond between Rh and amine is more stable with less sterically hindered ligands. Also such ligands can form complexes (**4′**) with both cationic amine and amine bonded with Rh, as it was proposed in work [18]. Species (**3**) is active in aldehyde hydrogenation. The activity of the hydride complexes with direct Rh-N bond in hydroformylation is debatable. We observed that less sterically hindered amines capable of formation of such complexes have stronger negative effect on hydroformylation activity compared to the hindered ones. The reason may be either the competition for the active Rh sites between such amines and olefins (f.e. formation of (**3′**) species) or low activity of species (**3**) in hydroformylation. Because of the formation of complexes (**3-3′**) and (**4-4′**), the systems with amine ligands presumably contain smaller quantity of (**1**) and (**2**), which are mostly responsible for hydroformylation.

The experiments in pure toluene with lower concentrations of Rh and amine (Fig. 5) showed the inhibition of hydroformylation in the cases of NMP-dine and NEt_3, but not *i*Bu_3N. Probably, under those conditions complex (**4**) is not formed because of lower polarity of the medium. We can not exclude the formation of polynuclear complexes with direct Rh-N bond, however, based on the results of XAS experiments and variation of Rh concentrations (Fig. 8) we assume that complex (**3**) or low nuclearity species are more active in aldehyde hydrogenation. Similar effect of phosphine ligands in the hydroformylation was observed upon EXAFS analysis in the work [44]. Rh-Rh bonds were registered at lower phosphine loadings and authors suggested formation a dirhodium diphosphine complex coexisting with monomeric complexes and clusters in the reaction mixture. They mention, though, that EXAFS describes the averaged Rh coordination sphere, so the mixture of monomeric and cluster complexes could not be excluded. This surely is relevant for the present study.

Here is to mention that solvent have a significant impact on the formation of either $Rh_6(CO)_{16}$ or $Rh_4(CO)_{12}$ complexes from $Rh_2(CO)_4Cl_2$ and CO [45]; they also have different solubility patterns: tetrarhodium cluster is well soluble in non-polar solvents, while hexarhodium one is not. In the series of *in situ* XAS experiments, we used high loadings of the amines to match high Rh content necessary for registration, so unpolar amines could additionally affect clusterization through the change in the polarity of the *i*PrOH-enriched medium.

4. Conclusions and future prospective

Tandem hydroformylation-hydrogenation of olefins is now considered as an important petrochemical process for the transformation of olefins into alcohols. For this, Rh/NR_3 systems are of considerable interest as catalysts, since in their presence the conversion proceeds in auto tandem mode, i.e. both stages – olefin hydroformylation and aldehyde hydrogenation – occur without change of the reaction conditions or catalyst alternation. In the present work, a number of amines with different substitutes were tested in Rh-catalyzed hydroformylation and aldehyde hydrogenation separately. Both electronic and steric properties of the amines were found to affect the hydrogenation stage. Catalytic and *in situ* XAS measurements shown that tertiary amines suppress Rh clusterization, forming numeric species of lower nuclearity. These Rh/amine species may include both charged and uncharged ones, the latter are believed to provide aldehyde hydrogenation. At the same time, addition of amines, which are effective promotors of the hydrogenation step, decelerates hydroformylation, presumably, through the formation of amine containing Rh complexes. Also, we demonstrated an implementation of high-pressure cell for *in situ* XAS studies as a powerful method for investigation of homogeneous catalysts under severe conditions. We believe that further research of structural insights, provided by *in situ* XAS methods, may be the key to complement high-pressure FTIR and NMR for better understanding the behavior of catalytic systems, such as Rh/NR_3 in reductive hydroformylation, as well as other industrially relevant reactions.

Declaration of Competing Interest

The authors declare that they have no known competing financial interests or personal relationships that could have appeared to influence the work reported in this paper.

Data availability

No data was used for the research described in the article.

Acknowledgments

This research was funded by the Ministry of Science and Higher Education of the Russian Federation, agreement No. 075-15-2021-1363. DG and MN acknowledges (partial) support from M.V. Lomonosov Moscow State University Program of Development for catalytic studies.

Appendix A. Supplementary data

The file with supporting information contains the reference list on *p*Ka data (Table S.1), data on oxygenates yields of in tandem hydroformylation-hydrogenation of hexene-1 vs *p*Ka of the amine ligands (fig. S.1), results of the tests of Rh/NR_3 in hydrogenation of some other substrates (Table S.2), results of catalytic experiments on hydroformylation and aldehyde hydrogenation in different solvents (fig. S.2), geometry optimization models of possible structures of the Rh complexes under syngas pressure obtained in DFT calculations (fig. S.3), and the results of experiments on aldehyde hydrogenation at different CO:H_2 ratios (Table S.3). Supplementary data to this article can be found online at https://doi.org/10.1016/j.jcat.2023.115194.

References

[1] H. Bahrmann, H. Bach, G.D. Frey, Oxo Synthesis, in: Ullmann's Encycl. Ind. Chem., Wiley-VCH Verlag GmbH & Co. KGaA, Weinheim, Germany, 2013, https://doi.org/10.1002/14356007.a18_321.pub2.

[2] J.K. MacDougall, D.J. Cole-Hamilton, Direct formation of alcohols in homogeneous hydroformylation catalysed by rhodium complexes, J. Chem. Soc. Chem. Commun. (1990) 165, https://doi.org/10.1039/c39900000165.

[3] J.K. MacDougall, M.C. Simpson, M.J. Green, D.J. Cole-Hamilton, Direct formation of alcohols by hydrocarbonylation of alkenes under mild conditions using rhodium trialkylphosphine catalysts, J. Chem. Soc. Dalt. Trans. (1996) 1161, https://doi.org/10.1039/dt9960001161.

[4] D. Fuchs, G. Rousseau, L. Diab, U. Gellrich, B. Breit, Tandem Rhodium-Catalyzed Hydroformylation-Hydrogenation of Alkenes by Employing a Cooperative Ligand System, Angew. Chemie Int. Ed. 51 (2012) 2178–2182, https://doi.org/10.1002/anie.201108946.

[5] L. Diab, T. Šmejkal, J. Geier, B. Breit, Supramolecular Catalyst for Aldehyde Hydrogenation and Tandem Hydroformylation-Hydrogenation, Angew. Chemie Int. Ed. 48 (2009) 8022–8026, https://doi.org/10.1002/anie.200903620.

[6] K. Takahashi, M. Yamashita, T. Ichihara, K. Nakano, K. Nozaki, High-Yielding Tandem Hydroformylation/Hydrogenation of a Terminal Olefin to Produce a Linear Alcohol Using a Rh/Ru Dual Catalyst System, Angew. Chemie Int. Ed. 49 (2010) 4488–4490, https://doi.org/10.1002/anie.201001327.

[7] K. Takahashi, M. Yamashita, K. Nozaki, Tandem Hydroformylation/Hydrogenation of Alkenes to Normal Alcohols Using Rh/Ru Dual Catalyst or Ru Single Component Catalyst, J. Am. Chem. Soc. 134 (2012) 18746–18757, https://doi.org/10.1021/ja307998h.

[8] G.M. Torres, R. Frauenlob, R. Franke, A. Börner, Production of alcohols via hydroformylation, Catal, Sci. Technol. 5 (2015) 34–54, https://doi.org/10.1039/C4CY01131G.

[9] D.N. Gorbunov, M.V. Nenasheva, M.V. Terenina, Y. Kardasheva, E.R. Naranov, A. L. Bugaev, A.V. Soldatov, A.L. Maximov, S. Tilloy, E. Monflier, E.A. Karakhanov, Phosphorus-free nitrogen-containing catalytic systems for hydroformylation and tandem hydroformylation-based reactions, Appl. Catal. A Gen. 647 (2022), 118891, https://doi.org/10.1016/j.apcata.2022.118891.

[10] S. Fuchs, D. Lichte, M. Dittmar, G. Meier, H. Strutz, A. Behr, A.J. Vorholt, Tertiary Amines as Ligands in a Four-Step Tandem Reaction of Hydroformylation and Hydrogenation: An Alternative Route to Industrial Diol Monomers, ChemCatChem 9 (2017) 1436–1441, https://doi.org/10.1002/cctc.201601518.

[11] D.L. Hunter, S.E. Moore, R.A. Dubois, P.E. Garrou, Deactivation of rhodium hydroformylation catalysts on amine functionalized organic supports, Appl. Catal. 19 (1985) 275–285, https://doi.org/10.1016/S0166-9834(00)81750-9.

[12] K. Cousin, B. Quienne, J. Pinaud, S. Caillol, E. Monflier, F. Hapiot, One-Pot Two-Step Synthesis of Hydroxymethylated Unsaturated VHOSO and Its Application to the Synthesis of Biobased Polyurethanes, Eur. J. Lipid Sci. Technol. 122 (2020) 2000158, https://doi.org/10.1002/ejlt.202000158.

[13] C. Becquet, M. Ferreira, H. Bricout, B. Quienne, S. Caillol, E. Monflier, S. Tilloy, Synthesis of diols from jojoba oil via rhodium-catalyzed reductive hydroformylation: a smart way to access biobased polyurethanes, Green Chem. 24 (2022) 7906–7912, https://doi.org/10.1039/D2GC02534E.

[14] J. Ternel, A. Lopes, M. Sauthier, C. Buffe, V. Wiatz, H. Bricout, S. Tilloy, E. Monflier, Reductive Hydroformylation of Isosorbide Diallyl Ether, Molecules 26 (2021) 7322, https://doi.org/10.3390/molecules26237322.

[15] M. Nenasheva, D. Gorbunov, M. Karasaeva, A. Maximov, E. Karakhanov, Non-phosphorus recyclable Rh/triethanolamine catalytic system for tandem hydroformylation/hydrogenation and hydroaminomethylation of olefins under biphasic conditions, Mol. Catal. 516 (2021), 112010, https://doi.org/10.1016/j.mcat.2021.112010.

[16] S. Püschel, E. Hammami, T. Rösler, K.R. Ehmann, A.J. Vorholt, W. Leitner, Auto-tandem catalytic reductive hydroformylation with continuous multiphase catalyst recycling, Catal. Sci. Technol. (2022), https://doi.org/10.1039/D1CY02000E.

[17] S. Püschel, J. Sadowski, T. Rösler, K.R. Ehmann, A.J. Vorholt, W. Leitner, Auto-Tandem Catalytic Reductive Hydroformylation in a CO 2 -Switchable Solvent System, ACS Sustain. Chem. Eng. 10 (2022) 3749–3756, https://doi.org/10.1021/acssuschemeng.2c00419.

[18] A. El Mouat, C. Becquet, J. Ternel, M. Ferreira, H. Bricout, E. Monflier, M. Lahcini, S. Tilloy, Promising Recyclable Ionic Liquid-Soluble Catalytic System for Reductive Hydroformylation, ACS Sustain. Chem. Eng. 10 (2022) 11310–11319, https://doi.org/10.1021/acssuschemeng.2c03302.

[19] D.N. Gorbunov, M.V. Nenasheva, E.A. Kuvandykova, S.V. Kardashev, E. A. Karakhanov, Promising Applications of Polyethyleneimine as a Ligand in Rhodium-Catalyzed Tandem Hydroformylation/Hydrogenation of Olefins, Pet. Chem. (2023), https://doi.org/10.1134/S0965544123030222.

[20] B. Corain, M. Basato, M. Zecca, G. Braca, A.M.R. Galletti, S. Lora, G. Palma, E. Guglielminotti, Direct synthesis of alcohols from n-olefins and syngas in the liquid phase catalyzed by rhodium supported on crosslinked acrylic resins, J. Mol. Catal. 73 (1992) 23–41, https://doi.org/10.1016/0304-5102(92)80059-P.

[21] D. Gorbunov, M. Nenasheva, E. Naranov, A. Maximov, E. Rosenberg, E. Karakhanov, Tandem hydroformylation/hydrogenation over novel immobilized Rh-containing catalysts based on tertiary amine-functionalized hybrid inorganic-organic materials, Appl. Catal. A Gen. 623 (2021), 118266, https://doi.org/10.1016/j.apcata.2021.118266.

[22] K. Kaneda, H. Kuwahara, T. Imanaka, New polymer-bound Rh carbonyl cluster catalysts containing two functional ligands for hydrohydroxymethylation of olefins, J. Mol. Catal. 72 (1992) L27–L30, https://doi.org/10.1016/0304-5102(92)85004-Y.

[23] B. Fell, A. Geurts, Hydroformylierung Mit Rhodiumcarbonyl-Tert.-Amin-Komplexkatalysatoren, Chemie Ing. Tech. - CIT 44 (1972) 708–712, https://doi.org/10.1002/cite.330441104.

[24] A.T. Jurewicz, L.D. Rolmann, D.D. Whitehurst, Hydroformylation with Rhodium-Amine Complexes, in: Adv. Chem., 1974: pp. 240–251. https://doi.org/10.1021/ba-1974-0132.ch016.

[25] Y.S. Varshavsky, T.G. Cherkasova, A simple method for preparing acetylacetonatodicarbonylrhodium (I), Russ. J. Inorg. Chem. 12 (1967) 1709–1712.

[26] A.A. Chernyshov, A.A. Veligzhanin, Y.V. Zubavichus, Structural Materials Science end-station at the Kurchatov Synchrotron Radiation Source: Recent instrumentation upgrades and experimental results, Nucl. Instruments Methods Phys. Res. Sect. A Accel. Spectrometers, Detect. Assoc. Equip. 603 (2009) 95–98, https://doi.org/10.1016/j.nima.2008.12.167.

[27] P.V. Shvets, P.A. Prokopovich, A.I. Dolgoborodov, O.A. Usoltsev, A.A. Skorynina, E.G. Kozyr, V.V. Shapovalov, A.A. Guda, A.L. Bugaev, E.R. Naranov, D. N. Gorbunov, K. Janssens, D.E. De Vos, A.L. Trigub, E. Fonda, M.B. Leshchinsky, V. R. Zagackij, A.V. Soldatov, A.Y. Goikhman, In Situ X-ray Absorption Spectroscopy Cells for High Pressure Homogeneous Catalysis, Catalysts 12 (2022) 1264, https://doi.org/10.3390/catal12101264.

[28] E. Naranov, A. Sadovnikov, O. Arapova, T. Kuchinskaya, O. Usoltsev, A. Bugaev, K. Janssens, D. De Vos, A. Maximov, The in-situ formation of supported hydrous ruthenium oxide in aqueous phase during HDO of lignin-derived fractions, Appl. Catal. B Environ. 334 (2023), 122861, https://doi.org/10.1016/j.apcatb.2023.122861.

[29] B. Ravel, M. Newville, ATHENA, ARTEMIS, HEPHAESTUS: data analysis for X-ray absorption spectroscopy using IFEFFIT, J. Synchrotron Radiat. 12 (2005) 537–541, https://doi.org/10.1107/S0909049505012719.

[30] S.I. Zabinsky, J.J. Rehr, A. Ankudinov, R.C. Albers, M.J. Eller, Multiple-scattering calculations of x-ray-absorption spectra, Phys. Rev. b. 52 (1995) 2995–3009, https://doi.org/10.1103/PhysRevB.52.2995.

[31] C. Fonseca Guerra, J.G. Snijders, G. te Velde, E.J. Baerends, Towards an order- N DFT method, Theor. Chem. Accounts Theory, Comput. Model. (theoretica Chim. Acta). 99 (1998) 391–403, https://doi.org/10.1007/s002140050353.

[32] J. Tao, J.P. Perdew, V.N. Staroverov, G.E. Scuseria, Climbing the Density Functional Ladder: Nonempirical Meta-Generalized Gradient Approximation Designed for Molecules and Solids, Phys. Rev. Lett. 91 (2003), 146401, https://doi.org/10.1103/PhysRevLett.91.146401.

[33] S. Grimme, J. Antony, S. Ehrlich, H. Krieg, A consistent and accurate ab initio parametrization of density functional dispersion correction (DFT-D) for the 94 elements H-Pu, J. Chem. Phys. 132 (2010), https://doi.org/10.1063/1.3382344.

[34] S. Grimme, S. Ehrlich, L. Goerigk, Effect of the damping function in dispersion corrected density functional theory, J. Comput. Chem. 32 (2011) 1456–1465, https://doi.org/10.1002/jcc.21759.

[35] T. Mizoroki, M. Kioka, M. Suzuki, S. Sakatani, A. Okumura, K. Maruya, Behavior of Amine in Rhodium Complex-Tertiary Amine Catalyst System Active for Hydrogenation of Aldehyde under Oxo Reaction Conditions, Bull. Chem. Soc. Jpn. 57 (1984) 577–578, https://doi.org/10.1246/bcsj.57.577.

[36] T. Rösler, K.R. Ehmann, K. Köhnke, M. Leutzsch, N. Wessel, A.J. Vorholt, W. Leitner, Reductive hydroformylation with a selective and highly active rhodium amine system, J. Catal. 400 (2021) 234–243, https://doi.org/10.1016/j.jcat.2021.06.001.

[37] C. Becquet, F. Berche, H. Bricout, E. Monflier, S. Tilloy, Hydrohydroxymethylation of Ethyl Ricinoleate and Castor Oil, ACS Sustain. Chem. Eng. 9 (2021) 9444–9454, https://doi.org/10.1021/acssuschemeng.1c02924.

[38] T. Mizoroki, K. Seki, S. Meguro, A. Ozaki, Rhodium Complex Catalyzed Hydrogenation of α, β-Unsaturated Aldehydes to Unsaturated Alcohols, Bull. Chem. Soc. Jpn. 50 (1977) 2148–2152, https://doi.org/10.1246/bcsj.50.2148.

[39] R.M. Laine, Criteria for identifying transition metal cluster-catalyzed reactions, J. Mol. Catal. 14 (1982) 137–169, https://doi.org/10.1016/0304-5102(82)80034-5.

[40] W. Simanko, K. Mereiter, R. Schmid, K. Kirchner, A.M. Trzeciak, J.J. Ziołkowski, Rh(acac)(CO)(PR 3) and Rh(oxinate)(CO)(PR 3) complexes—substitution chemistry and structural aspects, J. Organomet. Chem. 602 (2000) 59–64, https://doi.org/10.1016/S0022-328X(00)00118-2.

[41] G. Bor, Metal carbonyl clusters: thermodynamics of their formation and stability. Some novel results on cobalt, rhodium, ruthenium, and mixed clusters, Pure Appl. Chem. 58 (1986) 543–552, https://doi.org/10.1351/pac198658040543.
[42] D.H. Farrar, E.V. Grachova, A. Lough, C. Patirana, A.J. Poë, S.P. Tunik, Ligand effects on the structures of Rh6(CO)15L clusters, J. Chem. Soc. Dalt. Trans. (2001) 2015–2019, https://doi.org/10.1039/b010109p.
[43] N. Rosas, C. Márquez, H. Hernández, R. Gómez, Hydroformylation of cyclohexene under low pressure with Rh4(CO)12: evidence in favor of homogeneous cluster catalysis, J. Mol. Catal. 48 (1988) 59–67, https://doi.org/10.1016/0304-5102(88)85128-9.
[44] S.G. Fiddy, J. Evans, T. Neisius, X.-Z. Sun, Z. Jie, M.W. George, Extended X-ray absorption fine structure (EXAFS) characterisation of the hydroformylation of oct-1-ene by dilute Rh–PEt 3 catalysts in supercritical carbon dioxide, Chem. Commun. (2004) 676–677, https://doi.org/10.1039/B311331K.
[45] P. Chini, S. Martinengo, Synthesis of rhodium carbonyl compounds at atmospheric pressure. III. Synthesis of Rh4(CO)12 and of Rh6(CO)16, Inorganica Chim, Acta. 3 (1969) 315–318, https://doi.org/10.1016/S0020-1693(00)92502-7.